



ELSEVIER

Physica A 225 (1996) 294–311

**PHYSICA** A

# Multifractal processes and self-organized criticality in the large-scale structure of the universe

Pablo Garrido<sup>a</sup>, Shaun Lovejoy<sup>a</sup>, Daniel Schertzer<sup>b</sup>

<sup>a</sup>*Department of Physics, McGill University, 3600 University St., Montréal, H3A 2T8, Canada*

<sup>b</sup>*L.M.D., Université Pierre et Marie Curie, 4 Pl. Jussieu, F-75252, Paris Cedex 05, France*

Received 12 January 1995; revised 28 July 1995

---

## Abstract

In the past five to ten years mounting evidence has arisen indicating that the large-scale spatial number density of galaxies may be governed by fractal or multifractal statistics. In this paper we extend this idea by searching for multifractal behaviour in other density fields. Namely, generalized luminosity density fields (which we define here) constructed from information on both the angular position and the apparent luminosity of galaxies. Using data from the Center for Astrophysics' CfA2 catalogue, we perform various multifractal analyses that reveal that over broad angular scales, the fields studied present two important signatures of multifractal behavior: multiscaling and algebraic probability distributions associated with extreme fluctuations and first-order multifractal phase transitions. Since the presence of both of these phenomena is the defining feature of Self-Organized Criticality, we argue that the spatio-luminous distribution of galaxies in the observable universe may be described as a nonclassical self-organized critical phenomenon resulting from multifractal cascades.

*Keywords:* Galaxies; Multifractals; Scaling; Critical phenomena

---

## I. Introduction

### 1.1. Motivation

Statistical studies on the large-scale distribution of luminous objects in the universe have often reduced the problem to that of either a point distribution in space, or a functional variation in the luminosity probability distribution, independent of the spatial location. However, neither approach by itself is sufficient to completely describe – in a statistical sense – the observed universe. Results from the two-point galaxy correlation function  $\xi(r)$  (see for instance Peebles [1], Einasto et al. [2], Luo et al. [3], and Martinez [4]) have suggested that the spatial distribution of galaxies forms a fractal set of dimension  $\sim 1.23$  up to scales of the order of  $10 h^{-1}$  Mpc. However, more recent analyses (Coleman and Pietronero [5], Calzetti et al. [6]) have

shown that this upper limit of  $10 h^{-1}$  Mpc may be spurious since spatial homogeneity is apparently not reached within the scales of the samples studied. In such a case a mean space density cannot be well-defined, and consequently the upper scaling limit for  $\xi(r)$  becomes sample dependent. A similar effect may be observed if – as we argue here – the distribution of luminosity in the universe turns out to be multifractal with an outer scale greater than the sample size.

The main analytic tool in standard analyses of luminosity distributions has been the luminosity function  $\Phi(l)$ , which indicates the probability that within a given region of space, one finds a galaxy with an apparent luminosity in the range  $l$  to  $l + dl$ . Although various empirical fits have been proposed to the observed form of the luminosity function of several catalogues (see for instance Schechter [7], and Abell [8]) no convincing physical justification exists for the mathematical form of such fits. In addition, no connection has been made from such fits to the spatial distribution of galaxies.

Clearly, a complete statistical description of the large-scale distribution of galaxies must go beyond the treatment of galaxies as mathematical point objects and take into account other properties such as their mass and luminosity. In this paper, we propose that multifractals naturally provide such a unified framework, and quantitatively show that the largest publicly available catalogue of galactic luminosity is compatible with this framework up to the largest available angular scales.

In multifractal processes, the variability builds up step by step from the large to the small scales leading to high intermittence generally associated with algebraic probability tails and multifractal phase-transitions (as explained in section 3). Since the combination of scaling with algebraic probabilities can be regarded as the defining feature of Self-Organized Criticality (SOC), it has recently [20] been argued that such nonclassical SOC is a generic feature of multifractal processes. The corresponding multifractal phase transition route to SOC makes the specific prediction, which we verify in section 3 of this paper, that the normalized  $\eta$  powers of the luminosity fields will have critical exponents which vary according to a specific law, depending on a critical dimension which we estimate. More details can be found in Garrido [9].

### 1.2. Definition of the generalized apparent luminosity fields $l_{\eta,\lambda}$

In order to test the multifractal character of the universe at large scales, we define a family of generalized luminosity fields. These fields are constructed as follows: we first denote the standard information about a galaxy's angular position and apparent luminosity as  $l_A(\Omega)$ . The capital Greek letter  $A$  is the scale ratio of the largest to smallest scale in the sample, i.e. the maximum available spatial/angular resolution of the catalogue corresponding to an individual galaxy. The parameter  $\Omega$  represents the galaxy's angular position in spherical coordinates.

Next, consider a region of space  $A$  of size  $S$ . In order to define a field, this region is subdivided into  $i$  smaller regions  $B_{\lambda,i}$  of size  $s < S$  ( $s$  is an intermediate scale which defines the scale-ratio  $\lambda$  as  $\lambda \equiv S/s > 1$ ). The values of all the events  $l_A(\Omega)$  located

within each  $B_{\lambda,i}$  are raised to a power  $\eta$  and then summed up. We define the resulting sum as the “ $\eta$ -flux”  $\Pi^{(\eta)}(B_{\lambda,i})$  of the  $i$ th region at resolution  $\lambda$ . The “Generalized (apparent) Luminosity Field”  $l_{\eta,\lambda}(B_{\lambda,i})$  at resolution  $\lambda$ , is then defined as the density of the  $\eta$ -flux over the total volume (or area) of the region  $A$  under consideration:

$$\Pi^{(\eta)}(B_{\lambda,i}) \equiv \int_{B_{\lambda,i}} (l_A(\Omega))^\eta d\Omega, \quad l_{\eta,\lambda}(B_{\lambda,i}) \equiv \frac{\Pi^{(\eta)}(B_{\lambda,i})}{\text{Vol}(B_{\lambda,i})}. \quad (1)$$

$\text{Vol}(B_{\lambda,i})$  is a spatial/angular integral over the  $i$  regions  $B_{\lambda,i}$  within  $A$  (the subscript  $i$  runs between 1 and  $\lambda^D$ ,  $D$  being the dimension of the sample).

In our analysis, the fields  $l_{\eta,\lambda}(B_{\lambda,i})$  at resolution  $\lambda$  have been normalized so that  $\langle l_{\eta,\lambda}(B_{\lambda,i}) \rangle = 1$  (where the brackets  $\langle \rangle$  indicate ensemble average at resolution  $\lambda$  over the entire region  $A$ ). Note that a corresponding definition of the generalized absolute luminosity field  $L_{\eta,\lambda}$  is identical to Eq. (1), but with  $l_A(\Omega)$  replaced<sup>1</sup> by  $L_A(r, \Omega)$ . In this paper however, we concentrate solely on the analysis of  $l_{\eta,\lambda}$ . As it will be mentioned below, the analysis of  $L_{\eta,\lambda}$  requires additional considerations which will be properly discussed in a separate paper.

The systematic study of normalized  $\eta$  powers of a multifractal field (as given by Eqs. (1)) was first proposed by Lavallée [10]. However, with the partial exception of Coleman and Pietronero [11] (who studied  $\eta = 0, 1$ ) our research represents the first application of such a study to an astronomical field.

### 1.3. Some important members of the family of luminosity fields

The exponent  $\eta$  in Eqs. (1), indexes the member of the luminosity family under study. It can be noticed that  $l_{0,\lambda}$  represents the number density field of galaxies at scale-ratio  $\lambda$ . This field has been studied by Atmanspacher et al. [12] and Wiedenmann et al. [13] finding good evidence for multiscaling, often up to angular distances greater than  $30^\circ$  (in agreement with the large-scale inhomogeneities observed below in Fig. 2).  $l_{1,\lambda}$  represents the apparent luminosity field at scale  $\lambda$ ; that is, the (normalized) total amount of light received from all galaxies located within an angular region  $B_{\lambda,i}$  of extent  $s$ .

As mentioned earlier, in this paper we shall not analyze generalized fields  $L_{\eta,\lambda}$  of absolute luminosity. However, in order to help the reader gain familiarity with the concept of generalized luminosity fields, it is convenient at this point to give a physical interpretation of at least some fields  $L_{\eta,\lambda}$ . The three-dimensional number-density field of galaxies is represented by  $L_{0,\lambda}$ . Martinez [4], Jones et al. [14] and Dominguez-Tenreiro et al. [15] have shown that multifractals provide a good

<sup>1</sup> In order to simplify the notation in the rest of the analysis, the generalized luminosity fields will be written as  $l_{\eta,\lambda}$  and  $L_{\eta,\lambda}$ , so that their spatial dependence will be implicit.

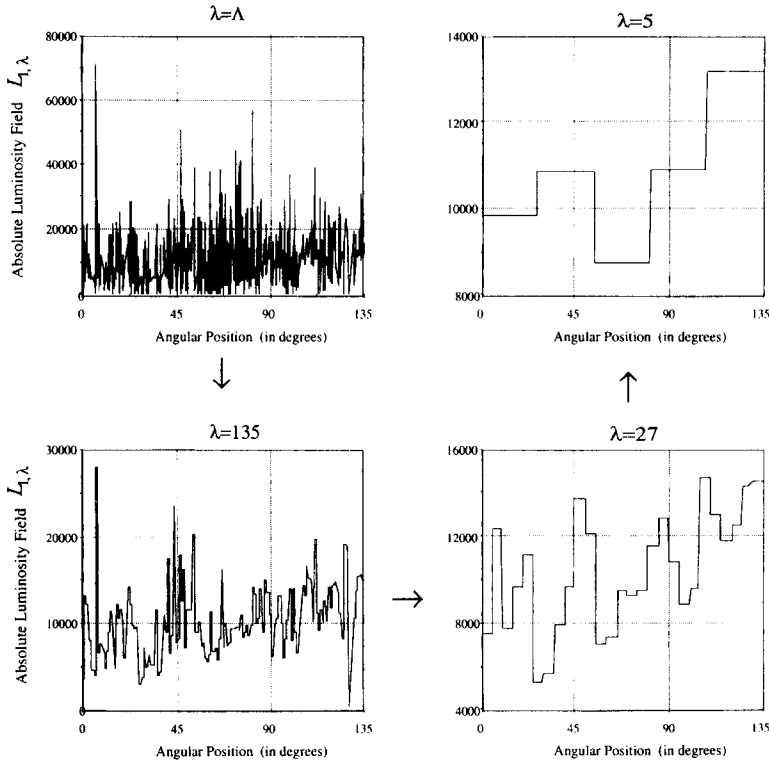


Fig. 1. Example of four fields  $L_{1,\lambda}$  as a function of the resolution  $\lambda$  for the sample CfA2proj (see discussion in text). The figures have been produced by averaging the luminosity over increasing angular scales. As the resolution decreases from the original raw-data ( $\lambda = A$ ) down to a resolution of  $27^\circ$  ( $\lambda = 5$ ), both variability and the intermittence of the field are observed to decrease severely. In order to facilitate the intercomparison among the figures, the luminosity fields were not normalized.

description of this field, at least for scales smaller than about  $10 h^{-1} \text{ Mpc}^2$ . Members of  $L_{\eta,\lambda}$  indexed by  $0.8 < \eta < 1.25$  (the exact value depending on the semi-empirical method used to relate absolute luminosity to mass) may be considered as estimates of the corresponding field of mass distribution. Coleman and Pietronero [5, 11], have recently analyzed the  $L_{1,\lambda}$  field finding good support for multifractality up to distances comparable with the size of the catalogues ( $\sim 50 \text{ Mpc}$ ). An example of a  $L_{1,\lambda}$  field is shown in Fig. 1. The data comes from the sample CfA2proj (discussed in the next section). It can be noticed that as the resolution decreases from  $\lambda = A$  to  $\lambda = 5$  (i.e. as

<sup>2</sup> In fact, we shall see that indeed the  $\eta = 0$  case has the poorest scaling since it is most sensitive to the low luminosity cut-off. See section 2.

<sup>3</sup> Since the angular resolution  $R$  of this catalogue is on the order of seconds of arc, and its maximum angular extent is  $135^\circ$  it follows that  $A = (135^\circ/R) \sim 10^5$ . See section on “data considerations”.

the luminosities are averaged over increasingly larger angles), the luminosity variation also decreases severely. Such behavior is typical of multifractal fields as will be explained below in Section 2.

Our research aims to develop Coleman and Pietronero's analysis further by exploring the multifractal properties of astronomical fields other than that given by  $\eta = 0$  and  $\eta = 1$ . By varying  $\eta$  it is possible to study the statistical features of the whole family of fields as a function of scale (or resolution). As  $\eta$  is increased, emphasis is placed on the extreme values of the field, whereas the opposite occurs as  $\eta$  is decreased. A theoretical reason for introducing the parameter  $\eta$  is that it conveniently allows us to test specific theoretical predictions about the underlying multifractal process, as it will be discussed in Section 3.

#### 1.4. Data considerations

To explore the statistics of the spatio/luminous distribution of visible mass in the universe, it would be ideal to analyze data of the three dimensional distribution of absolute luminosity fields. Actual galaxy catalogues however, do not contain such information. They often contain data only on the angular position and the apparent magnitude of galaxies. Information on apparent luminosity can be readily derived from the observed magnitudes. Radial distances are usually deduced using Hubble's law. However, this requires an extra measurement; namely, that of the redshift associated with each galaxy. Absolute luminosities are then derived using both the inferred radial distance, and the measured apparent luminosity. Unfortunately, estimates of the radial distances are often subject to considerably uncertainty due to a variety of factors, which range from practical considerations such as a galaxy's peculiar motion in space, to profound theoretical arguments that question the validity of Hubble's law.

Moreover, three dimensional samples of absolute luminosity suffer from the Malmquist bias, that is, the existence of a distance dependent minimum threshold for the visual observation of faint galaxies. Standard techniques of by-passing the Malmquist bias consider either constructing volume-limited samples (i.e. sub-samples with a constant threshold of absolute luminosity  $L_{1,A}$ ) or invoking functions such as the luminosity function  $\Phi(L)$  to predict the luminosity of the unobserved galaxies. Unfortunately, neither solution is completely satisfactory since the former severely reduces the number of galaxies available for analysis (which is already small in a statistical sense), and the latter is based on theoretical assumptions about the form of the luminosity distribution and its validity everywhere in space, (neglecting any possible spatial correlations).

On the other hand, data samples constructed from information only on angular position and apparent luminosity do possess a constant minimum luminosity threshold and are hence statistically homogeneous over all solid angles. Furthermore, if the apparent luminosities are indeed multifractal fields then the effect that the Malmquist bias has on them is identical to that caused by the existence of a minimum

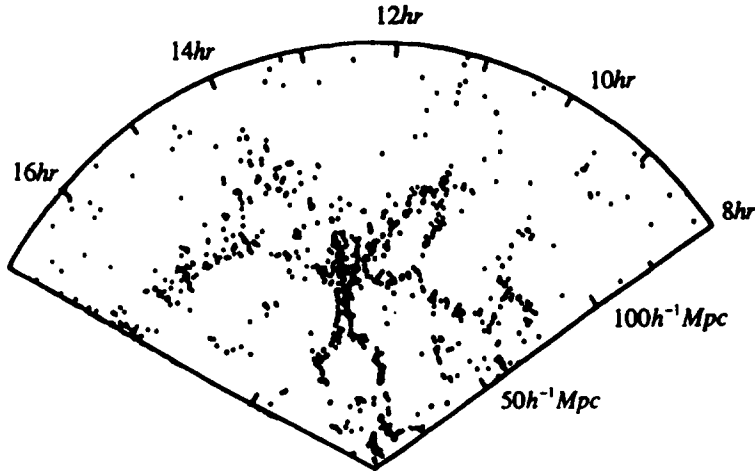


Fig. 2. The CfA2 catalogue [16]: a “Slice of the Universe”. The figure displays 1091 galaxies with apparent magnitude  $m \leq 15.5$  located in the region  $8 \text{ hr} \leq \alpha \leq 17 \text{ hr}$  and  $26^\circ.5 \leq \delta \leq 32^\circ.5$ . The sample’s depth is  $150 h^{-1} \text{ Mpc}$  ( $h$  is in units of  $100 \text{ km s}^{-1} \text{ Mpc}^{-1}$ ). The large voids observed show the existence of inhomogeneous structures at scales comparable with the catalogue’s size.

threshold (or singularity), rather than a complex distance dependent effect. Larnder [16] has shown that the problem of minimum thresholds in multifractal fields can be analyzed in a straightforward way. Finally, the fact that samples constructed from information on angular position and apparent luminosity consider just directly measurable quantities, maximizes the accuracy of the data. Due to these facts (which are sometimes overlooked) we have decided to limit our analysis to generalized luminosity fields  $l_{\eta,\lambda}$  derived from apparent luminosity. Furthermore, as pointed out by Garrido [9], the line of sight integration that relates the fields  $L_{\eta,\lambda}$  and  $l_{\eta,\lambda}$  assures – with suitable statistical assumptions to be discussed elsewhere- that the statistics of the fields of apparent luminosity can be related to the statistics of the three dimensional distribution of absolute luminosity.

In our analysis, we used a modified version of the catalogue CfA2 (Huchra et al. [17]) from the Harvard-Smithsonian Center for Astrophysics (see Fig. 2). In its original form, the CfA2 sample contains 1091 galaxies with apparent magnitude less than or equal to 15.5 located within a  $6^\circ$  by  $135^\circ$  strip passing through the Coma cluster. The sample is  $150 \text{ Mpc}$  deep and is bounded by the angular positions  $8 \text{ hr} \leq \alpha \leq 17 \text{ hr}$  and  $26^\circ.5 \leq \delta \leq 32^\circ.5$  (where  $\alpha$  denotes right ascension and  $\delta$  is the declination). This “slice of the universe” contains information on the luminosity and position of galaxies in radial and angular coordinates.

The sample that we have used in our analysis (from now on called “CfA2proj”) is a one-dimensional projection (along constant right ascension  $\alpha$ ) of the CfA2 sample. It hence contains information only on the angular position and luminosity of the galaxies. An example of a luminosity field constructed with data from the CfA2proj

sample was already shown in Fig. 1. The reason for producing such a one-dimensional projected sample is that since there is only a finite (and statistically small) number of galaxies in the catalogue, it is expected that the luminosity fields will become ill-defined at scales corresponding to densities close to 1 galaxy per box (at such densities, most boxes will in fact be empty), hence inducing breaks in the scaling which will be spurious since they will depend on the catalogue's sensitivity. On the other hand, for a fixed resolution  $\lambda$ , a field projected along one of its spatial coordinates increases its average number of galaxies per box by a factor of  $\lambda$ , thus also increasing the range of scales within which scaling may be observed. This leads to much more robust statistics. In fact, analysis performed by Garrido [9] on the unprojected CfA2 catalogue shows that although his results are compatible to ours, the sample CfA2 presents scaling ranges significantly shorter than the corresponding ranges for the sample CfA2proj.

As previously stated, in their original forms catalogues contain information on the apparent magnitude  $m$  of the galaxies. In our analysis, the values of the corresponding apparent luminosities  $l$  were obtained using

$$l = 10^{(m' - m)/2.5}, \quad (2)$$

where  $m'$  is the limiting magnitude of the catalogue.

## 2. Multiscaling and the multifractal formalism

Highly intermittent multifractal fields are the generic outcome of multiplicative cascade processes dominated by scaling non-linear interactions. Such cascading processes appear to be fairly common in nature (over a dozen geophysical fields have been shown to be multifractal over various ranges, see Schertzer and Lovejoy [18] for a survey) and in the specific case of the large-scale structure of the universe, most theories on the formation of galaxies also suggest their existence (for instance, both the "Hot" and "Cold" dark matter models require the existence of a cascade of energy and matter ruled by complex non-linear gravitational and hydrodynamical interactions). When a multifractal cascade has proceeded over a scale ratio  $\lambda \equiv S/s$  ( $S$  being the sample's size and  $s$  the smallest scale of observation) the statistical moments of the conserved luminosity field  $l_{\eta,\lambda}$  measured at scale  $\lambda$ , follow the singular behavior:

$$\langle (l_{\eta,\lambda})^q \rangle = \lambda^{K(q,\eta)}, \quad (3)$$

where the exponent  $q$  is the order of the statistical moment under study, and the quantity  $K(q,\eta)$  is the moment-scaling function<sup>4</sup> corresponding to the (base  $\lambda$ ) second

<sup>4</sup> We use the codimension multifractal formalism since we consider the observed universe as a realization of an infinite dimensional stochastic multifractal process. The exponent  $K(q,\eta)$  is related to the strange attractor dimension formalism (Halsey et al. [19]) by  $\tau(q) = (q - 1)D - K(q, 1)$  where  $D$  is the dimension of the observing space.

Laplace characteristic function of the field  $\log(l_{\eta,\lambda})$ . The triangular brackets  $\langle \rangle$  in Eq. (3) denote a statistical ensemble average which is calculated over the number  $\tilde{N}_\lambda$  of non-empty boxes<sup>5</sup> at resolution  $\lambda$  using the formula:

$$\langle (l_{\eta,\lambda})^q \rangle = (1/\tilde{N}_\lambda) \sum_{i=1}^{\tilde{N}_\lambda} (l_{\eta,\lambda})_i^q \tag{4}$$

Eq. (3) is the mathematical definition of multiscaling. In Fig. 3 we show plots of  $\log_{10} \langle (l_{\eta,\lambda})^q \rangle$  versus  $\log_{10}(\lambda)$  for  $\eta = 0, 1, 2$  and  $3$ . According to Eq. (3), for a multifractal field these plots should give straight lines. In general this seems to be the case, although only for a limited range of scales. The most restricted scaling range is observed for  $\eta = 0$  corresponding to the most frequently analyzed field (the number density of galaxies<sup>6</sup>). In this case, the scaling region extends from  $\lambda \approx 4$  to  $\lambda \approx 128$ , implying angular scaling between  $1^\circ$  and about  $35^\circ$  (recall that the maximum extent of this sample is  $135^\circ$ ). For higher  $\eta$ 's, the scaling region extends from  $35^\circ$  down to about  $0.13^\circ$  ( $\lambda \approx 1024 \approx$  total number of galaxies) which is about the largest possible for a data set of this size.

For all values of the exponent  $\eta$  in Fig. 3, deviations from linearity are also observed within the scaling regions. This result is not surprising due to the statistically low number of events used in this analysis (recall that the total number of galaxies in this catalogue is 1091). Also, since multifractals display large sample to sample variability (they are generally nonergodic<sup>7</sup>) and since here we consider only a single realization of the multifractal luminosity process, the statistical fluctuations in Fig. 3 are generally expected. Consequently, although multiscaling seems to be observed in all fields studied, the poor statistics derived from the available catalogues are expected to introduce significant uncertainties on the estimates of the function  $K(q, \eta)$ .

For a monofractal,  $K(q, \eta)$  is simply linear in  $q$ , whereas for multifractal fields,  $K(q, \eta)$  is nonlinear. In general,  $K(0, \eta) = -C$  where  $C$  is the codimension of the nonzero regions ( $= 0$  here, the latter are space-filling) and for a conservative field Eq. (3) predicts that  $K(1, \eta) = 0$ . Moreover, since  $K(q, \eta)$  mathematically corresponds to the second characteristic function of a field it follows that it must be convex. Furthermore, for high  $\eta$  values the largest singularities of the field are amplified and so are the corresponding estimates of the ensemble average in Eq. (3). Consequently  $K(q, \eta)$  is expected to become steeper for increasing<sup>8</sup>  $\eta$ .

<sup>5</sup> The difference between  $\tilde{N}_\lambda$  and  $N_\lambda$  (the total number of boxes at resolution  $\lambda$ ) is  $\lambda^{-C}$  where  $C$  is the fractal codimension of the non-empty boxes. The non-empty boxes used here highlight the nonlinear part of  $K(q, \eta)$ .

<sup>6</sup> This may not be too surprising since the measured density will depend sensitively on the limiting magnitude cut-off of the catalogue; and since the lowest singularities are most important for low values of  $\eta$ , it is expected that such a cut-off will break the scaling.

<sup>7</sup> Multifractal cascades generally produce occasional rare events which may not be present in a single sample, but which are almost surely present in the process. The effect is especially important when there are first order phase transitions with low values of the critical exponent -exactly as found here (Section 3).

<sup>8</sup> In general, it obeys the following simple relation:  $K(q, \eta) = K(q\eta, 1) - qK(\eta, 1)$ , see e.g. Ref. [18].



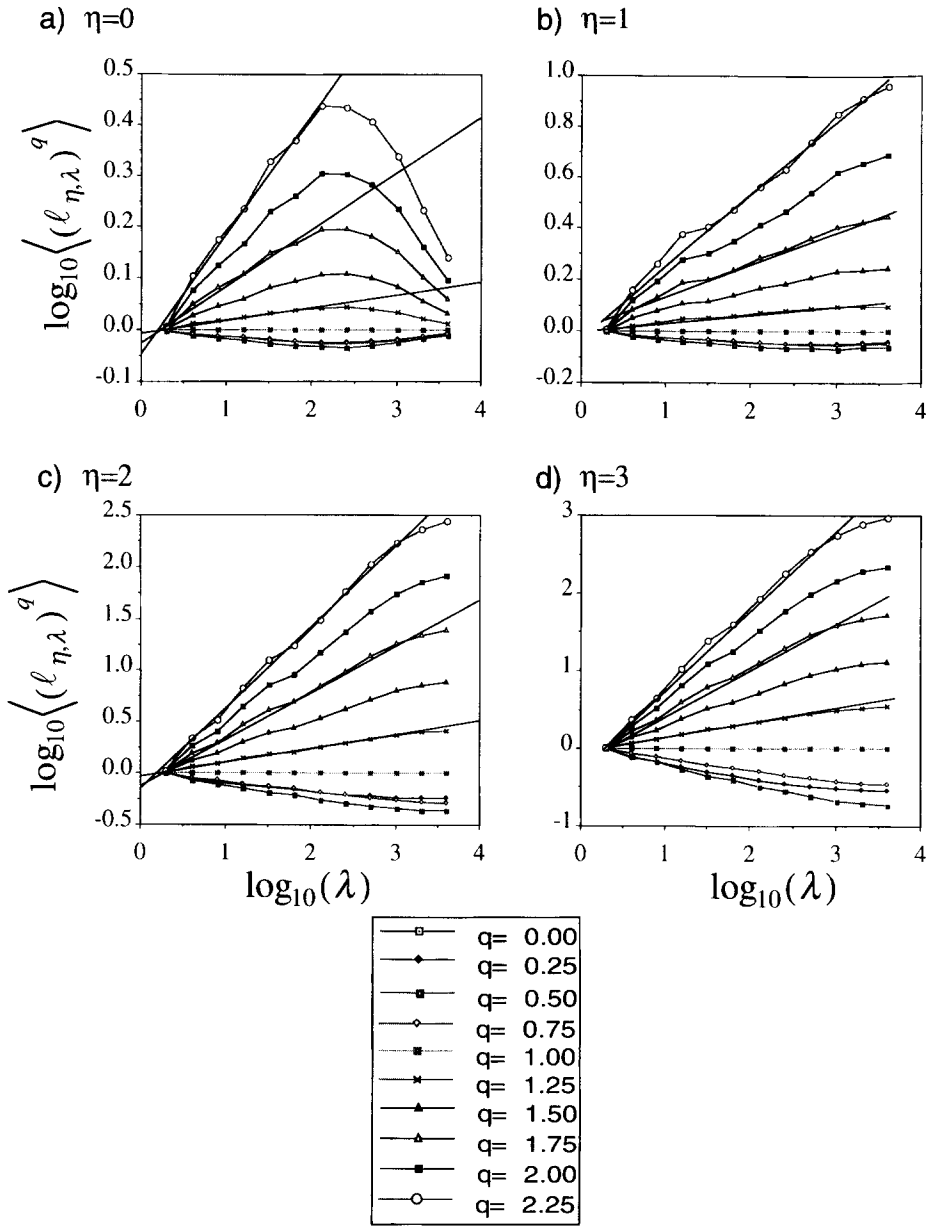


Fig. 3. Multiscaling of four  $l_{\eta, \lambda}$  fields as predicted by Eq. (3). The values of  $\eta$  are 0, 1, 2 and 3. The analysis shown corresponds to the 1091 galaxies from the CfA2proj sample. Angular scaling regions are clearly observed in all of the fields. In each figure, each curve corresponds to a specific value of  $q$ . We have used  $0 \leq q \leq 2.25$ , in intervals of 0.25.

For a given pair of  $\eta$  and  $q$ , we have estimated  $K(q, \eta)$  from the value of the slopes in Fig. 3. These slopes have been estimated using a linear regression over the linear

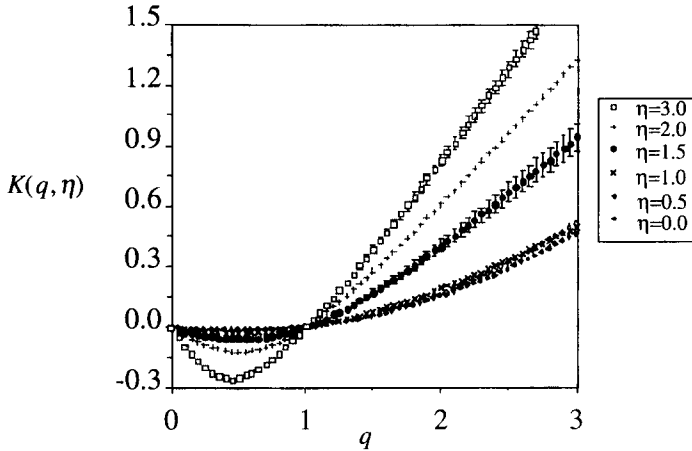


Fig. 4.  $K(q, \eta)$  for the multiscaling curves of figure 3. In this figure we have also shown the results corresponding to  $\eta = 0.5$  and  $\eta = 1.5$ . The number-density field ( $\eta = 0$ ), the apparent luminosity field ( $\eta = 1$ ) and all of the other  $\eta$ -fields show strong convexity, in agreement with the predictions from multifractality.

scaling region of the curves. The estimated values of  $K(q, \eta)$  are shown in Fig. 4 for  $\eta = 0; 0.5; 1; 1.5; 2$  and  $3$ . Error bars were estimated from the standard deviation of the slope fits, and in order to preserve the clarity of the figure, they are just shown for  $\eta = 1.5$  and  $3.0$ . The curves are far from linear showing strong convexity (a good signature of multifractality) for all fields  $l_{\eta, \lambda}$ .

The results presented above are a generalization of the results found by previous studies (Refs. [4, 12–15]) on the multifractal features of the number-density field (the  $\eta = 0$  case) and comparable studies (Refs. [5, 11]) done on the distribution of absolute luminosity ( $L_{i, \lambda}$ ). Furthermore, these results suggest that the physical processes responsible for the spatial distribution of luminous objects in the universe are multifractal. It is natural to ask whether multifractal processes have stable, attractive generators; after a long debate, (see e.g. the discussion in [20]) it is increasingly clear that the answer is affirmative. Elsewhere<sup>9</sup> evidence is given that suggests that the luminosities correspond to universal multifractals.

It could be argued that the  $K(q, \eta)$  shown in Fig. 4 may be sensitive to the angular projection (line of sight integration) performed when constructing the sample CfA2proj. To show that this is not so, we “projected” the CfA2 catalogue along constant radii (rather than angles) obtaining scaling ranges similar to those observed in Fig. 3 and similar  $K(q, \eta)$ . Fig. 5 describes the two kinds of projections. Figs. 6a, b show the results of this analysis (for reasons of space and clarity, we just show the

<sup>9</sup> See Garrido [9].

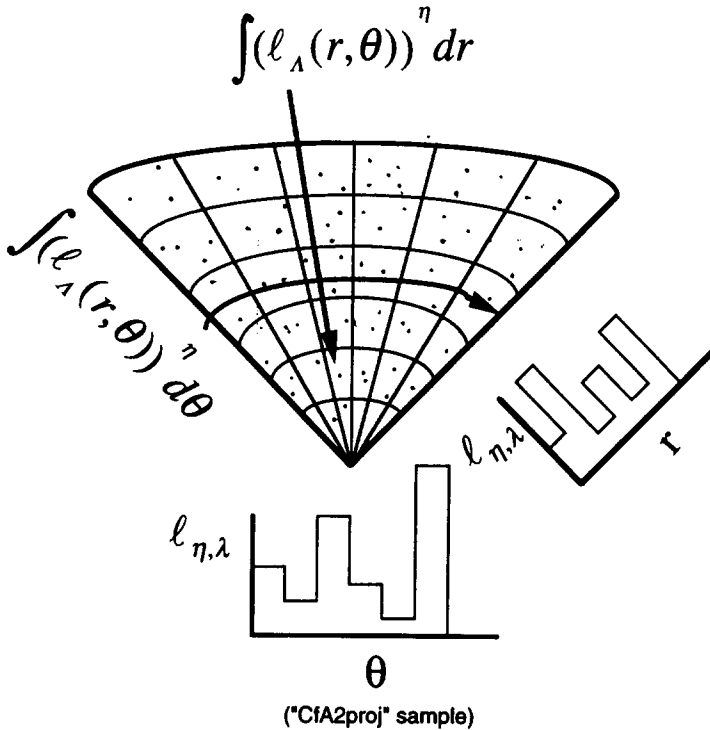


Fig. 5. Schematic showing the construction of projected samples. Using the CfA2 catalogue as the data source, the sample CfA2proj is obtained by the angular integration of the luminosities along the radial direction. Analysis of a field constructed by integrating instead along the angular coordinate  $\theta$ , revealed scaling properties very similar to those displayed by the CfA2proj sample. This indicates that the scaling observed in the latter sample is not an artifact of the angular integration.

results corresponding to the  $\eta = 1$  case. Analyses performed on fields with  $\eta \neq 1$  are compatible with what is shown here). Fig. 6a shows the multiscaling of the field  $l_{1, \lambda}$  as obtained from a sample obtained by projecting the CfA2 catalogue along constant radii. Broad scaling regions (very similar to those observed in Fig. 3b for the same field) can be clearly observed. Fig. 6b shows the  $K(q, 1)$  curves corresponding to both projected fields. The agreement of the statistical functions for both projections is clear<sup>10</sup>. This agreement suggests that angular and cartesian projections possess similar scaling properties. It also implies that, in particular, the broad scaling regions observed in Fig. 3 are not due to the angular projection of the CfA2proj sample.

<sup>10</sup> Small differences occur for  $q \geq q_{D,1} \approx 1.33$ , but this is expected since the corresponding moments diverge, as shown in the next section.

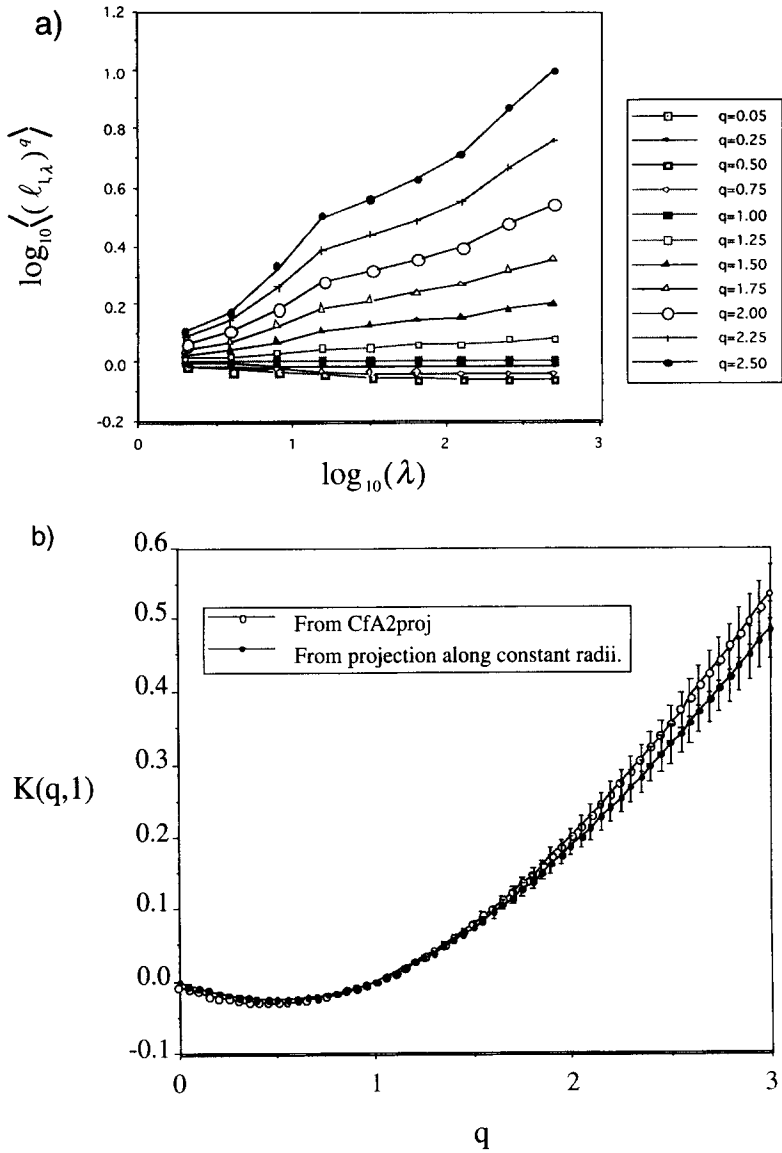


Fig. 6. (a) Multiscaling of the field  $l_{v,z}$  as obtained from a projection of the sample CfA2 along constant radii (not along constant angles as for the sample CfA2proj). Each curve corresponds to a specific value of  $q$ . (b)  $K(q, 1)$  curves estimated from the two projected subsamples of the sample CfA2. The similarity between the statistics of both projections implies that the broad scaling regions observed in Figs. 3 and 5a are not sensitive to the nature of the projection of the luminosity fields. The curves in Fig. 5b were obtained from linear regressions on the slopes of the scaling region of the curves shown in Figs. 3b and 5a.

### 3. Multifractal phase transitions and self-organized criticality

The notion of Self-Organized Criticality (SOC) was first introduced by Bak et al. [22] as an explanation to the  $1/f$  noise detected in various dynamical systems. Although different authors have emphasized different aspects, scaling coupled with algebraic probability distributions can be considered as the defining features of Self-Organized Criticality. Schertzer and Lovejoy [18, 19] have pointed-out that these properties are generically obtained on multifractal processes via a “first-order multifractal phase transition” (as explained below)<sup>11</sup>. Since in the previous section we already showed that the generalized luminosity fields  $l_{\eta,z}$  display multiscaling over broad ranges of scales, in this section we concentrate on the presence of power-law behavior in the extreme tails of the probability distributions of the fields  $l_{\eta,z}$ .

As previously stated, multifractal fields are the generic result of multiplicative cascading processes of conserved energy fluxes. As a cascading process develops down to very small scales, the variability and intermittence of the field increases producing regions of highly localized extreme intensity (recall for instance the extreme variability observed in Fig. 1). Generally, such cascading processes are truncated at some small scale limit at which external scale-breaking mechanisms (such as viscosity in turbulent fluids) dissipate the energy of the cascade. Since such a physical small scale limit is usually smaller than the scale of observation (at which actual measurements of the field are performed), the process of observation effectively integrates or averages the field up to the scale of observation. For the non-extreme events, this integrated or “dressed” field has the same scaling as the actual “bare” field [23]. However, in the case of the more violent and extreme singularities of the field, the integration fails to smooth out the process inducing peculiar behaviour on the large  $q$  end of the function  $K(q, \eta)$ . In fact, for orders of moment greater than some critical value denoted as  $q_{D, \eta}$  (the subscript D standing for dressing), the ensemble average in Eq. (3) is expected to diverge to infinity (for an infinitely large sample) implying that  $K(q, \eta) \rightarrow \infty$  for  $q > q_{D, \eta}$ . In practice, for a finite sample size and observing dimension, the dressing mechanism induces a linear behaviour in  $K(q, \eta)$  for  $q$  larger than  $q_{D, \eta}$  (as observed for large  $q$  in the plots of Fig. 4) with a slope dependent on the sample size. This linear form implies a change on the first derivative of  $K(q, \eta)$  at  $q = q_{D, \eta}$ . Due to the formal analogy between thermodynamics and multifractals (see for instance Feigenbaum [24]), this type of jump on the derivative of  $K(q, \eta)$  has been named a first order multifractal phase transition. Note that this definition of phase transition is physically different from the multifractal phase transitions usually discussed in the physics literature since the latter typically correspond to scale-breaking mechanisms. In contrast, the concept of phase transition presented here is fundamentally a scaling mechanism dependent on the sample size and the dimension of the observing space.

<sup>11</sup> Such a “non-classical” SOC has the advantage of being both model independent and not requiring a vanishing flux [18].

Although the above described result is quite general for multifractal processes, it is possible to consider – as it is often done – special multifractal processes restricted in various ways so that the most extreme multifractal variability is inhibited and the divergence of moments avoided. One way is to use the microcanonical restriction, as for example in the “p model” and the “two-scale Cantor set model”. Another is the use of “geometric multifractals”, as proposed by Parisi and Frisch [25]. These artificial restrictions have been discussed in detail by Schertzer and Lovejoy [26].

The behaviour of the various statistical moments of a field is statistically equivalent to the behaviour of its probability distribution. In general, the divergence of moments for  $q \geq q_{D,\eta}$  implies that the tail of the probability distribution obeys the following form

$$\Pr(l_{\eta,\lambda} \geq s) \approx s^{-q_{D,\eta}}, \tag{5}$$

where  $s$  is some reference value and  $s \gg 1$ . Indeed, a linear tail on a log–log plot of a probability histogram is probably the most sensitive way to distinguish first order from other types of phase transitions (namely, second order phase transitions discussed in Ref. [21]).

Fig. 7 shows a plot<sup>12</sup> of  $\log_{10}(\Pr(l_{\eta,\lambda} \geq s))$  versus  $\log_{10}(s)$  for  $\eta = 1, 2$  and  $3$ . In each case,  $q_{D,\eta}$  is obtained from the value of the slope of the histogram’s tail. In particular, we estimate that  $q_{D,1} = 1.33 \pm 0.05$ ,  $q_{D,2} = 0.64 \pm 0.06$  and  $q_{D,3} = 0.36 \pm 0.04$ . In this case all histograms were taken at a resolution  $\lambda = 128$  which is well within the scaling range of this sample (see Fig. 3).

By inspecting Eq. (5), we note that the right hand side shows no explicit dependence on the resolution  $\lambda$  of the field. This is because the exponent  $q_{D,\eta}$  should be resolution-independent as shown in Fig. 8. It can be noticed from this figure that the value of  $q_{D,1} \approx 1.35$  remains roughly constant even for very large values of  $\lambda$ .

The generic cascade mechanism leading to first order transitions is the dressing integration mechanism discussed earlier. In terms of multifractal theory, such a mechanism makes the specific prediction (Schertzer and Lovejoy [18]) that the quantity  $q_{D,\eta}$  corresponds to the solution of the following equation:

$$K(q_{D,\eta}, \eta) = D(q_{D,\eta} - 1), \tag{6}$$

where  $D$  is a proportionality constant interpreted as the effective dimension of the space over which the “dressing” takes place. Eq. (6) is a specific prediction of the multifractal phase transition route to Self-Organized Criticality and generalizes the corresponding equation for  $\eta = 1$  in Ref. [23]. It is also a test on the dressing-mechanism hypothesis for the presence of first order multifractal phase transitions in the distribution of generalized luminosity fields.

---

<sup>12</sup>The probabilities have been estimated from the number of boxes in the field at resolution  $\lambda$  which have generalized luminosities greater than a reference value  $s$ .

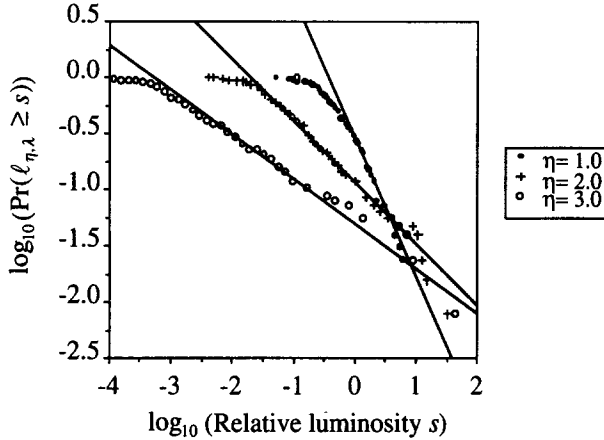


Fig. 7. Probability histograms for three fields  $l_{\eta,\lambda}$ . The slopes of the linear regions provide estimates of the quantity  $q_{D,\eta}$ , which varies as a function of  $\eta$ .  $\lambda = 128$  in all cases.

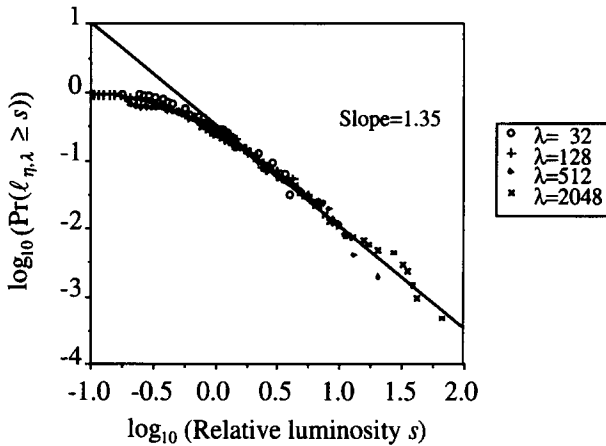


Fig. 8. Independence of  $q_{D,\eta}$  on the resolution  $\lambda$ : for four different values of  $\lambda$ , the probability histograms (plotted against normalized probabilities) show a consistent estimate of  $q_{D,1} \sim 1.35$ .

We have used the data from the sample CfA2proj to calculate the quantities  $q_{D,\eta}$  and  $K(q_{D,\eta}, \eta)$  for values of  $\eta$  ranging between zero and three. Fig. 9 shows the plot of  $K(q_{D,\eta}, \eta)$  versus  $q_{D,\eta} - 1$ . This figure shows a nearly linear curve that passes through the origin and with a slope  $D = 0.45 \pm 0.06$ . This linear behaviour is in agreement with Eq. (6) and it is therefore interpreted as further evidence for the presence of Self-Organized Criticality, whose origin lies in the cascade dressing process, in the generalized fields of galactic luminosity. The physical significance of the dressing dimension  $D$  is that it indicates the existence of some physical mechanism

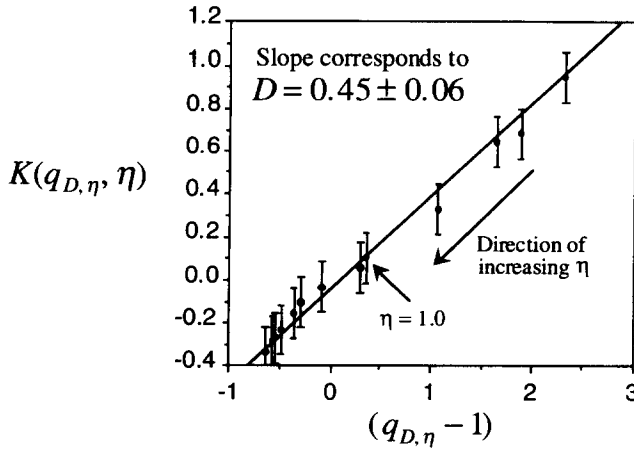


Fig. 9.  $K(q_{D,\eta}, \eta)$  versus  $(q_{D,\eta} - 1)$  as estimated from the sample CfA2proj for 13 values of  $\eta$  in the range  $[0, 3]$ . The linear behavior observed in this figure is in agreement with Eq. (8) and provides further evidence for the presence of Self-Organized Criticality in the luminosity fields  $l_{\eta,z}$ .

which “integrates” or “smoothes out” the dynamical process responsible for the luminosity field on a space with a dimension  $\sim 0.45$ . Similar analyses applied to seismic fields (Hooge et al. [27]) have also indicated the presence of this type of non-classical phase transition route to SOC.

#### 4. Conclusions

It has long been known that the large-scale structure of the universe is scale invariant over a substantial range. In this paper we extended this idea by generalizing the work of Coleman and Pietronero [5] and introducing the concept of generalized luminosity fields  $l_{\eta,z}$ . We then showed that the galaxy catalogue CfA2 (involving over 1000 galaxies) produces luminosity fields which indeed display multiscaling over the entire observed angular range. In the  $\eta = 0$  case however, a more restricted scaling range was observed. This is not too surprising since number-density fields are expected to be most sensitive to the existence of a lower threshold cut-off. This fact however, reflects a convenient feature of the use of generalized luminosity fields as analytic tools; namely the fact that rather than studying single fields (which would have led us to wrong conclusions had we only considered the  $\eta = 0$  field) the use of generalized fields exploits the statistical information conveyed by all members of the family of fields  $l_{\eta,z}$ .

A generic feature of multifractal processes is that they lead to first order multifractal phase transitions originating in the sub-observation scale dynamics. These multifractal phase transitions involve occasional large fluctuations and are associated



with algebraic decays of the corresponding probability distributions. In the case of the generalized luminosity fields, the existence of large fluctuations corresponds to the existence of rare but extremely bright or massive galaxies which tend to dominate the statistics and cause power-law probability distributions. Since the combination of algebraic probability tails (divergence of high order statistical moments) with scaling can be considered as the defining feature of Self-Organized Criticality, this suggests that the observed spatio-luminous distribution of galaxies is statistically compatible with multifractal fields formed via models of multiplicative cascades of energy and mass, whose statistics can be described in terms of a set of self-organized critical exponents. In particular, our results suggest that nonlinear galactic dynamics is an example of such a (nonclassical) multifractal phase transition route to SOC. Further support for this view can be obtained because the multifractal phase transition route to SOC makes a specific prediction about the critical exponents  $q_{D,\eta}$  associated with the (normalized)  $\eta$  powers of the luminosity (cf. Eq. (6)). This prediction is indeed well verified by the data and allows us to estimate the effective dimension of the “dressing” or “smoothing” of the underlying dynamic process.

In the context of the Big-Bang theory, two of the most popular scenarios which have been postulated as candidates for leading up to the formation of the large-scale structure of the universe are the “Hot” and “Cold” dark matter scenarios. Both scenarios imply the existence of cascading processes of non-linear gravitational and hydrodynamical clustering of energy and matter. The former scenario predicts that the cascade has developed from very large structures down to smaller ones, whereas the latter scenario postulates the opposite cascading direction. Since the direction of the cascading process is indeterminate from our analysis, the hypothesis of a multifractal cascade as a route to the large-scale luminosity clustering is compatible with either the Hot or the Cold models.

In summary, we have found evidence supporting the idea that the large-scale distribution of luminous objects in the universe may be the result of a multifractal cascade process. This process seems to have been “dressed” or “smoothed” in a subspace of dimension  $\sim 0.45$  which causes the statistics of the resulting fields (of galactic density, luminosity, mass, etc.) to be ruled by critical exponents (c.f. Eqs. (5) and (6)). Such a description implies in particular that large-scale inhomogeneous and clustered structures (such as the so-called “filaments”, “bubbles”, “pancakes” and “walls” found in recently published catalogues [17, 28, 29]) should be common features of the universe, rather than exceptions. A future task then, is to incorporate our knowledge on both multifractals and critical phenomena (with all its implications on the scale-invariance of the underlying dynamics) into the metric which describes the observable universe.

## References

- [1] P.J.E. Peebles, *Physica D* 38 (1989) 273.
- [2] J. Einasto, A.A. Klypin and E. Saar, *M.N.R.A.S.* 219 (1986) 457.

- [3] X. Luo, and D.N. Schramm, *Science* 256 (1992) 513.
- [4] V.J. Martinez, in: *Applying Fractals to Astronomy*, eds. A. Heck and J.M. Perdgang (Springer, Berlin, 1991) p. 135.
- [5] P.H. Coleman and L. Pietronero, *Phys. Rep.* 213 (1992) 311.
- [6] D. Calzetti, M. Giavalisco, R. Ruffini and G. Wiedenmann, *Astron. Astrophys.* 251 (1991) 385.
- [7] P. Schechter, *Astrophys J.* 203 (1976) 297.
- [8] G.O. Abell, *Annu. Rev. Astron Astrophys.* 3 (1965) 1.
- [9] P. Garrido, M. Sc. Thesis, McGill University, Canada (1994) [79 pages].
- [10] D. Lavallée, Ph.D. Thesis, McGill University, Canada (1991) [133 pages].
- [11] P.H. Coleman and L. Pietronero, *Physica A* 185 (1992) 45.
- [12] H. Atmanspacher, H. Scheingraber and G. Wiedenmann, *Phys. Rev. A* 40 (1989) 3954.
- [13] G. Wiedenmann and H. Atmanspacher, *Astron. Astrophys.* 229 (1990) 283.
- [14] B.J.T. Jones, V.J. Martinez, E. Saar and J. Einasto, *Astrophys. J.* 332 (1988) L1.
- [15] R. Dominguez-Tenreiro and V.J. Martinez, *Astrophys. J.* 389 (1989) L9.
- [16] C. Larnder, M.Sc. Thesis, McGill University, Canada (1995) [101 pages].
- [17] J.P. Huchra, M. Geller, V. de Lapparent and H. Corwin, *Astrophys. J. Lett.* 72 (1990) 433.
- [18] D. Schertzer and S. Lovejoy, in: *Fractals in the Natural and Applied Sciences*, ed. M.M. Novak (North-Holland, Amsterdam, 1994) pp. 325; *Phys. Rep.*, in press.
- [19] T.C. Halsey, M.H. Jensen, L.P. Kadanoff and I. Procaccia, *Phys. Rev. A* 33 (1986) 1141.
- [20] D. Schertzer, S. Lovejoy, D. Lavallée and F. Schmitt, in: *Nonlinear Dynamics of Structures*, eds. R.Z. Sagdeev, U. Frisch, F. Hussain, S.S. Moiseev and N.S. Erokhin (World Scientific, Singapore, 1991) pp. 213–235.
- [21] D. Schertzer, S. Lovejoy and D. Lavallée, in: *Cellular Automata: Prospects in Astrophysical Applications*, eds. J.M. Perdgang and A. Lajeune (World Scientific, Singapore, 1993) p. 216.
- [22] P. Bak, C. Tang and K. Wiesenfeld, *Phys. Rev. Lett.* 59 (1987) 381.
- [23] D. Schertzer and S. Lovejoy, *J. Geoph. Res.* 92 (1987) 9693.
- [24] J.F. Feigenbaum, *J. of Stat. Phys.* 46 (1987) 5.
- [25] G. Parisi and U. Frisch, in: *Turbulence and Predictability in Geophysical Fluid Dynamics and Climate Dynamics*, eds. M. Ghil, R. Benzi, G. Parisi (North-Holland, Amsterdam, 1985).
- [26] D. Schertzer and S. Lovejoy, *Physica A* 185 (1992) 187.
- [27] C. Hooge, S. Lovejoy, D. Schertzer, S. Peckold, J.F. Malouin and F. Schmitt, *Nonlinear Proc. Geophys.* 1 (1994) 191.
- [28] S.S.R.S. Survey, L.N. Da Costa, P.S. Pellegrini, L.W. Sargent, J. Tonry, M. Davis, A. Meiksin, D.W. Latham, J.W. Menzies and I.A. Coulson, *Astrophys. J.* 327 (1988) 544.
- [29] APM Galaxy Survey, S.J. Maddox, G. Efstathiou, W.J. Sutherland and J. Loveday, *M.N.R.A.S.* 242 (1990) 43.